

Geometrically nonlinear analysis of functionally graded porous beams

Şeref D. Akbaş*

Department of Civil Engineering, Bursa Technical University, Yıldırım Campus, Yıldırım, Bursa 16330, Turkey

(Received March 21, 2017, Revised December 5, 2017, Accepted April 20, 2018)

Abstract. In this paper, geometrically non-linear analysis of a functionally graded simple supported beam is investigated with porosity effect. The material properties of the beam are assumed to vary through height direction according to a prescribed power-law distributions with different porosity models. In the nonlinear kinematic model of the beam, the total Lagrangian approach is used within Timoshenko beam theory. In the solution of the nonlinear problem, the finite element method is used in conjunction with the Newton-Raphson method. In the study, the effects of material distribution such as power-law exponents, porosity coefficients, nonlinear effects on the static behavior of functionally graded beams are examined and discussed with porosity effects. The difference between the geometrically linear and nonlinear analysis of functionally graded porous beam is investigated in detail. Also, the effects of the different porosity models on the functionally graded beams are investigated both linear and nonlinear cases.

Keywords: geometrically nonlinear analysis; functionally graded material; porosity; total Lagrangian; finite element method

1. Introduction

Functionally graded materials (FGMs) are a new generation of composites whose composition varies continuously as a function of position along thickness of a structure to achieve a required function. FGMs are generally made of a mixture of ceramic and metal to satisfy the demand of ultra-high-temperature environment and to eliminate the interface problems. Typically, in an FGM, one face of a structural component is ceramic that can resist severe thermal loading and the other face is metal which has excellent structural strength. FGMs consisting of heat-resisting ceramic and fracture-resisting metal can improve the properties of thermal barrier systems because cracking and delamination, which are often observed in conventional layered composites, are reduced by proper smooth transition of material properties. The technology of FGMs was an original material fabrication technology proposed in Japan in 1984 by Sendai Group. Since the concept of FGMs has been introduced in 1980s, these new kinds of materials have been employed in many engineering application fields, such as aircrafts, space vehicles, defense industries, electronics and biomedical sectors, to eliminate stress concentrations, to relax residual stresses, and to enhance bonding strength. Because of the wide material variations and applications of FGMs, it is important to study the responses of FGM structures to mechanical and other loadings.

In recent years, with the development of technology, increasing demands for optimum or minimum-weight designed structural components makes it necessary to use non-linear theory of beams. Many optimum or minimum-

weight designed structural components are under severe operational conditions. In many cases, the small deflection linear theory is no longer applicable. It is very necessary to use and understand crack and fracture behaviour with non-linear analysis.

In the open literature, there are many studies in the linear analysis of the functionally graded beams. However, nonlinear studies of functionally graded beams are very limited. In the literature, studies of the nonlinear behavior of beams are as follows; The thermal buckling load of a curved beam made of FGM with doubly symmetric cross section was investigated by Rastgo *et al.* (2005). Agarwal *et al.* (2006) analysed the large deformation behaviour of anisotropic and inhomogeneous beams using exact linear static solutions. Li *et al.* (2006) examined the thermal post-buckling of FGM clamped-clamped Timoshenko beams subjected to transversely non-uniform temperature. Based on Kirchhoff's assumption of straight normal line of beams and considering the effects of the axial elongation, the initial curvature and stretching-bending coupling on the arch deformation, geometrically nonlinear governing equations of FGM arches subjected to mechanical and thermal loads were derived by Song and Li (2008). Kang and Li (2009) studied the bending of FGM cantilever beams with power-law non-linearity subjected to an end force. Ke *et al.* (2009) investigated the post-buckling of FGM beams with an open edge crack based on the Timoshenko beam theory and von Kármán nonlinear kinematics by using the Ritz method. Kang and Li (2010) examined the large deflections of a non-linear cantilever FGM beam. The thermal post-buckling behaviour of uniform slender FGM beams was investigated independently using the classical Rayleigh-Ritz formulation and versatile finite element analysis based on the von Karman strain-displacement relations by Anandrao *et al.* (2010). Kocatürk *et al.* (2011) investigated the full geometrically non-linear static analysis

*Corresponding author, Associate Professor
E-mail: serefd@yaho.com

of a cantilever Timoshenko beam composed of FGM under a non-follower transversal uniformly distributed load. Fallah and Aghdam (2011) studied the nonlinear free vibration and post-buckling analysis of FGM beams on nonlinear elastic foundation. Almeida *et al.* (2011) conducted the geometric nonlinear analyses of FGM beams by using a tailored Lagrangian formulation. The thermomechanical stability of FGM thin-walled cantilever pipes conveying flow and loading by compressive axial force was investigated by Hosseini and Fazlzadeh (2011). Li and Li (2011) analyzed post-buckling behavior of FGM columns under distributed loads. Yan *et al.* (2012) investigated the nonlinear flexural dynamic behavior of a clamped Timoshenko beam made of FGM with an open edge crack under an axial parametric excitation, composed of a static compressive force and a harmonic excitation force based on the Timoshenko beam theory and von Kármán nonlinear kinematics.

Mohanty *et al.* (2012) studied static and dynamic stability of FGM ordinary and sandwich beams by using finite element method based on the Timoshenko beam theory. Kocatürk and Akbaş (2012) presented the post-buckling analysis of FGM Timoshenko beams made of functionally graded material under thermal loadings. Akbaş and Kocatürk (2013) presented post-buckling analysis of FGM three-dimensional beams under the influence of temperature. Kocatürk and Akbaş (2010, 2011, 2013), Akbaş and Kocatürk (2012) investigated the nonlinear analysis of FGM and homogenous beams. Akbaş (2013) presented the geometrically nonlinear static analysis of edge cracked FGM Timoshenko beams subjected to a non-follower transversal point load. Nonlinear bending and thermal post-buckling of FGM beams resting on an elastic foundation investigated by (Hui-Shen and Wang (2014), Li and Shao (2014), Zhang and Zhou (2014), Sun *et al.* (2016), Trinh *et al.* (2016)). Babilio (2014) investigated the nonlinear dynamics of FGM beams resting on a linear viscoelastic foundation under the axial time-dependent excitation. Nguyen *et al.* (2014) analyzed geometrically nonlinear of FGM planar beam and frame structures by using finite element method. Ebrahimi and Salari (2015) investigated free vibration and buckling of FGM size-dependent nanobeams based on nonlocal elasticity theory of Eringen and the physical neutral axis position by using a semi-analytical differential transform method. Akbaş (2015a, b) analyzed post-buckling of cracked and axially graded FGM beams. Elmaguiri *et al.* (2015) studied the large-amplitude free vibration of clamped immovable thin FGM beams. Kolakowski and Teter (2015) studied static coupled buckling of thin-walled FGM columns with trapezoidal and square cross-sections. Akbaş (2013b, 2014a, b, 2015a, b, c, d, 2017a, b, 2018b, c) investigated nonlinear, vibration post-buckling of FGM and composite structures. Amara *et al.* (2016) investigated post-buckling of simply supported FGM beams using various shear deformation theories. Akbarzadeh Khorshidi *et al.* (2016) analyzed post-buckling of shear deformable FGM nanobeams based on modified couple stress theory with von-Karman geometric nonlinearity.

Porosity is a measuring of the voids in the space of the

materials. Porosity is defined as a fraction of the volume of voids over the total volume in the material, and its value varies between 0 and 1. During the processing in the fabrication of functionally graded materials, it can occur micro-voids and porosities in the material body due to technical problems, curing or poor quality productions. Especially, the part of ceramic in the functionally graded materials occurs voids more frequently. After the production, porosities and voids can increase in the material depending on environmental and other conditions. It is known that porosities in structural materials introduces a low-strength, becomes more low-strength and its mechanical behaviors will be changed seriously. Therefore, the effect of the porosity must be considered in the safe design of the FGM structures.

In the literature, studies of the porosity effect in the FGM structures are as follows; Wattanasakulpong and Ungbhakorn (2014) studied linear and nonlinear vibration FGM beams with porosity effects. Mechab *et al.* (2016a, b) examined free vibration analysis of a FGM nano-plate resting on elastic foundations with the porosities effect. Yahia *et al.* (2015) studied wave propagation of FGM porous plates with different plate theories. Şimşek and Aydın (2017) examined forced vibration of FGM microplates with porosity effects based on the modified couple stress theory. Mouaici *et al.* (2016) studied free vibration of FGM porous plates within hyperbolic shear deformation theory. Ebrahimi and Habibi (2016b) investigated deflection and vibration of porous plates by using finite element method. Benferhat *et al.* (2016b) analyzed static behavior of FGM porous plates by using a new refined plate theory. Benferhat *et al.* (2016a) examined static and vibration of FGM porous plates resting on Winkler-Pasternak foundations. Jahwari and Naguib (2016) investigated FGM viscoelastic porous plates with a higher order plate theory and statistical based model of cellular distribution. Vibration analysis of FGM beams with porosity effect are investigated by (Ebrahimi and Jafari (2016a, b), Ebrahimi *et al.* (2016), Atmane *et al.* (2015a, b), Hadji *et al.* (2015), Ebrahimi and Salari (2015a, b), Ebrahimi *et al.* (2015), Hadji and Bedia (2015), Hadji (2016, 2017), Hadji *et al.* (2017), Bellifa *et al.* (2016), Galeban *et al.* (2016), Ebrahimi and Barati (2016a, b, c), Ebrahimi and Farzamandnia (2016), Ebrahimi and Hosseini (2016), Zouatnia *et al.* (2017), Akbaş (2017c, d, e, f, g, 2018a)).

As seen from literature, post-buckling behavior of FGM beams with porosity effects has not been investigated so far. The primary purpose of this study is to fill this gap for FGM beams. It is seen from literature that geometrically nonlinear behavior of FGM beams with porosity effects has not been investigated so far. The primary purpose of this study is to fill this gap for FGM beams. The distinctive feature of this study from previous study for the author Akbaş (2013) is investigation the porosity effect in the geometrically nonlinear analysis of FGM Timoshenko beams. A better understanding of the mechanism of how the porosity and material distribution change response of nonlinear behavior FGM beam is necessary, and is a prerequisite for further exploration and application of the

FGM beams. In the present study, the geometrically nonlinear static analysis of a FGM Timoshenko beam studied with porosity effect by using the total Lagrangian finite element method by taking into account full geometric nonlinearity.

The effects of material distribution and porosity parameters on the nonlinear static responses FGM beams are investigated with different porosity models. Also, the difference between the geometrically linear and nonlinear analysis of FGM porous beam is investigated in detail.

2. Theory and formulation

A simple supported FGM beam of length L , width b , and height h , as shown in Figure 1. One of the supports of the beam is assumed to be pinned and the other is rolled. The beam is subjected to a transversal point load (F) at the midpoint of the beam in the transverse direction as seen from Fig. 1. The FGM beam is made porous materials and vary though height direction. It is assumed that the bottom surface of the FGM beam is metal rich, whereas the top surface of the FGM beam is ceramic rich.

The effective material properties of the FGM beam, P , i.e., Young's modulus E , Poisson's ratio ν and shear modulus G vary continuously in the thickness direction (Y axis) according to a power-law function as follows

$$P(Y) = (P_c - P_m) \left(\frac{Y}{h} + \frac{1}{2} \right)^k + P_m \quad (1)$$

where P_m and P_c are the material properties of the metal and the ceramic surfaces of the beam, k is the non-negative power-law exponent which dictates the material variation profile through the thickness of the beam. It is clear from Eq. (1) that when $Y=-h/2$, $P=P_m$, and when $Y=h/2$, $P=P_c$. When $k=0$ (full ceramic) or $k=\infty$ (full metal), the material of the beam is homogeneous. according to Eq. (1).

In the porosity effect for imperfect FGM beam, two porosities models (even and uneven) are used which were given by Wattanasakulpong and Ungbhakorn (2014) for the power law distribution. In the first porosity model (even), the porosity spread uniformly though height direction. In the second porosity model (uneven), the porosity spread functionally though height direction. The distributions of the even and uneven porosity distributions are shown in Fig. 2.

According to the power law distribution, the effective material property for the even porosity can be expressed as follows

$$P(Y, a) = (P_c - P_m) \left(\frac{Y}{h} + \frac{1}{2} \right)^k + P_m - (P_m + P_{BC}) \frac{a}{2} \quad (2)$$

where a ($a \ll 1$) is the volume fraction of porosities. When $a=0$, the beam becomes perfect FGM. For uneven porosity distribution, the effective material property can be expressed as follows according to the power law distribution

$$P(Y, a) = (P_c - P_m) \left(\frac{Y}{h} + \frac{1}{2} \right)^n + P_m - (P_m + P_c) \frac{a}{2} \left(1 - \frac{2|Y|}{h} \right) \quad (3)$$

In the comparison of the two models: In uneven porosity model, the voids stack in the middle of the beam or the neutral of the beam. So, the stiffness of the cross-section is less effected from negative influences of the porosity because the neutral axis and its adjacent areas have low stress. However, the voids stack uniformly in the whole area of the beam in the even porosity model. Hence, the stiffness of the cross-section seriously decreases seriously in the even model. As result, the rigidity of the beam in even porosity model is lower than the rigidity of the beam in uneven porosity model.

In the nonlinear kinematic model of the beam, the total Lagrangian approach is used within Timoshenko beam theory. The Lagrangian formulations of the problem are developed for porosity FGM beam by using the formulations given by Felippa (2017) for isotropic and homogeneous beam material. The finite beam element of the problem is derived by using a two-node beam element shown in Fig. 3, of which each node has three degrees of freedom, i.e., two displacements u_{xi} and u_{yi} , and one rotation θ_i about the Z axis.

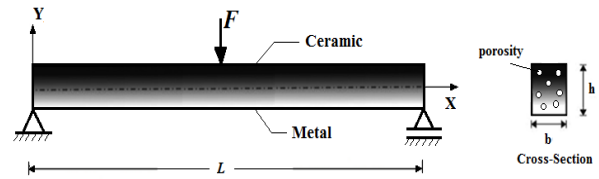


Fig. 1 A simple supported FGM beam with porosity subjected to a non-follower transversal point load

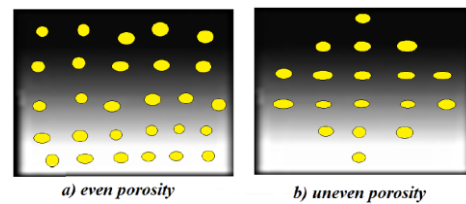


Fig. 2 Porosity models for FGM material

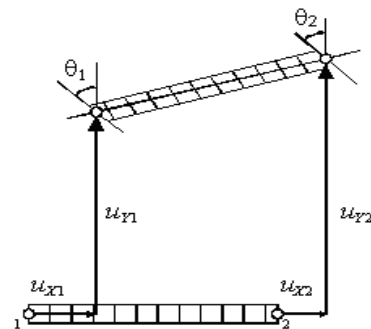


Fig. 3 Two-node C^0 beam element

In the deformation process, a generic point of the beam located at $P_0(X, Y)$ in the previous configuration C_0 moves to $P(x, y)$ in the current configuration C , as shown in Fig. 4. The projections of P_0 and P along the cross sections at C_0 and C upon the neutral axis are called $C_0(X, 0)$ and $C(x_0, y_0)$, respectively. It is assumed that the cross section of the beam remains unchanged, such that the shear distortion $\gamma \ll 1$ and $\cos \gamma$ can be replaced by 1 Felippa (2017).

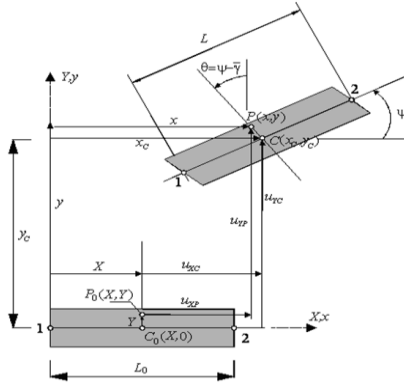
The coordinates of the beam at the current C configuration are

$$\begin{aligned} x &= x_c - Y(\sin\psi + \sin\gamma \cos\psi) \\ &= x_c - Y[\sin(\psi + \gamma) + (1 - \cos\psi)\sin\psi] \\ &= x_c - Y\sin\theta \end{aligned} \quad (4)$$

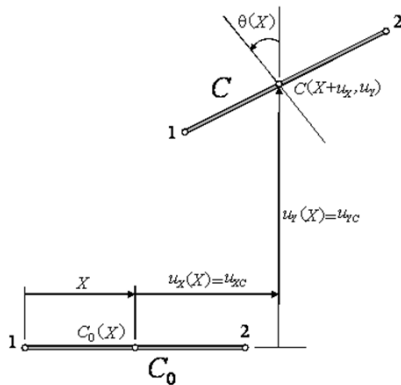
$$\begin{aligned} y &= y_c + Y(\cos\psi - \sin\gamma \sin\psi) \\ &= y_c + Y[\cos(\psi + \gamma) + (1 - \cos\gamma)\cos\psi] \\ &= y_c + Y\cos\theta \end{aligned} \quad (5)$$

where, $x_c = X + u_{XC}$ and $y_c = u_{YC}$. Consequently, $x = X + u_{XC} - Y\sin\theta$ and $y = u_{YC} + Y\cos\theta$. From now on, we shall call u_{XC} and u_{YC} simply u_X and u_Y , respectively. Thus the Lagrangian representation of the coordinates of the generic point at C is

$$\begin{bmatrix} x \\ y \end{bmatrix} = \begin{bmatrix} X + u_X - Y\sin\theta \\ u_Y + Y\cos\theta \end{bmatrix} \quad (6)$$



(a) Motion of plane beam



(b) Reduction to one-dimensional element

Fig. 4 Lagrangian kinematics of the C^0 beam element with X -aligned reference configuration Felippa (2017)

in which u_X , u_Y and θ are functions of X only. This concludes the reduction to a one-dimensional model, as sketched in Fig. 4(b). For a two-node C_0 element, it is natural to express the displacements and rotation as linear functions of the node degrees

$$\begin{bmatrix} u_X(X) \\ u_Y(X) \\ \theta(X) \end{bmatrix} = \frac{1}{2} \begin{bmatrix} 1-\xi & 0 & 0 & 1+\xi & 0 & 0 \\ 0 & 1-\xi & 0 & 0 & 1+\xi & 0 \\ 0 & 0 & 1-\xi & 0 & 0 & 1+\xi \end{bmatrix} \begin{bmatrix} u_{X1} \\ u_{Y1} \\ \theta_1 \\ u_{X2} \\ u_{Y2} \\ \theta_2 \end{bmatrix} = \mathbf{N}\mathbf{u} \quad (7)$$

in which $\xi=(2X/L_0)-1$ is the isoparametric coordinate that varies from $\xi=-1$ at node 1 to $\xi=1$ at node 2.

The Green-Lagrange strains are given as follows Felippa (2017)

$$\begin{aligned} [\mathbf{e}] &= \begin{bmatrix} e_1 \\ e_2 \end{bmatrix} = \begin{bmatrix} e_{XX} \\ 2e_{XY} \end{bmatrix} \\ &= \begin{bmatrix} (1 + u'_X)\cos\theta + u'_Y \sin\theta - Y\theta' - 1 \\ 2e_{XY} \end{bmatrix} = \begin{bmatrix} e - Y\kappa \\ \gamma \end{bmatrix} \end{aligned} \quad (8)$$

$$e = (1 + u'_X)\cos\theta + u'_Y \sin\theta - Y\theta' - 1$$

$$\gamma = (1 + u'_X)\sin\theta + u'_Y \cos\theta; \quad \kappa = \theta' \quad (9)$$

where e is the axial strain, γ is the shear strain, and κ is curvature of the beam, $u'_X = X/dX$, $u'_Y = du_Y/dX$, $\theta' = d\theta/dX$. By assuming that the material of the FGM beam obeys Hooke's law, the second Piola-Kirchhoff stresses in the beam become

$$\mathbf{S} = \begin{bmatrix} S_{XX} \\ S_{XY} \end{bmatrix} = \begin{bmatrix} S_1 \\ S_2 \end{bmatrix} = \begin{bmatrix} s_1^0 + E(Y, a)e_1 \\ s_2^0 + G(Y, a)e_2 \end{bmatrix} = \mathbf{s}^0 + \mathbf{E}\mathbf{e} \quad (10)$$

where E is the modulus of elasticity, G is the shear modulus and their dependence on the Y coordinate and porosity parameter a are given by Eqs. (2) and (3) with porosity effect. Using the constitutive equations, the axial force N , shear force V and bending moment M can be obtained as

$$\begin{aligned} N &= \int_A s_1 dA = \int_A s_1^0 + E(Y, a)(e - Y\kappa) dA \\ &= N^0 + (A_{xx}e - B_{xx}\kappa \end{aligned} \quad (11)$$

$$\begin{aligned} V &= \int_A s_2 dA = \int_A s_2^0 + E(Y, a)e_2 dA \\ &= V^0 + A_{xz}\gamma \end{aligned} \quad (12)$$

$$\begin{aligned} M &= \int_A -Ys_1 dA = \int_A -Y(s_1^0 + E(Y, a)e_1) dA \\ &= M^0 - B_{xx}\kappa + A_{xx}e + D_{xx}\kappa \end{aligned} \quad (13)$$

where

$$N^0 = \int_A s_1^0 dA, \quad V^0 = \int_A s_2^0 dA, \quad M^0 = \int_A -Ys_1^0 dA \quad (14)$$

$$(A_{xx}, B_{xx}, D_{xx}) = \int_A E(Y, a)(1, Y, Y^2) dA \quad (15)$$

$$A_{xz} = \int_A G(Y, a) dA = \int_A \frac{E(Y, a)}{2(1+\nu(Y, a))} dA \quad (16)$$

with $(A_{xx}, B_{xx}, D_{xx}$ and A_{xz} denoting the extensional, coupling, bending, and transverse shear rigidities respectively, ν is Poisson ratio.

For the solution of the geometrically nonlinear problem in the total Lagrangian coordinates, a small-step incremental approach based on Newton-Raphson iteration method is used. In the Newton-Raphson solution for the problem, the applied load is divided by a suitable number of increments according to its value. After completing an iteration process, the previous accumulated load is increased by a load increment.

The solution for the $n+1$ st load increment and i th iteration is performed using the following relation

$$d\mathbf{u}_n^i = (\mathbf{K}_T^i)^{-1} \mathbf{R}_{n+1}^i \quad (17)$$

where \mathbf{K}_T^i is the tangent stiffness matrix of the system at the i th iteration, $d\mathbf{u}_n^i$ is the displacement increment vector at the i th iteration and $n+1$ st load increment, $(\mathbf{R}_{n+1}^i)_S$ is the residual vector of the system at the i th iteration and $n+1$ st load increment. This iteration procedure is continued until the difference between two successive solution vectors is less than a preset tolerance in the Euclidean norm, given by

$$\sqrt{\frac{[(d\mathbf{u}_n^{i+1} - d\mathbf{u}_n^i)^T (d\mathbf{u}_n^{i+1} - d\mathbf{u}_n^i)]^2}{[(d\mathbf{u}_n^{i+1})^T (d\mathbf{u}_n^{i+1})]^2}} \leq \xi_{tol} \quad (18)$$

A series of successive iterations at the $n+1$ st incremental step gives

$$\mathbf{u}_{n+1}^{i+1} = \mathbf{u}_{n+1}^i + d\mathbf{u}_{n+1}^i \quad (19)$$

where

$$\Delta \mathbf{u}_n^i = \sum_{k=1}^i d\mathbf{u}_n^k \quad (20)$$

The residual vector \mathbf{R}_{n+1}^i for the structural system is given as follows

$$\mathbf{R}_{n+1}^i = \mathbf{f} - \mathbf{p} \quad (21)$$

Where \mathbf{f} is the vector of total external forces and \mathbf{p} is the vector of total internal forces, as given in the Appendix.

The element tangent stiffness matrix for the total Lagrangian Timoshenko beam element as given by Felippa (2017) is

$$\mathbf{K}_T = \mathbf{K}_M + \mathbf{K}_G \quad (22)$$

where \mathbf{K}_G is the geometric stiffness matrix, and \mathbf{K}_M is the material stiffness matrix given as follows

$$\mathbf{K}_M = \int_{L_0} B_m^T S B_m dX \quad (23)$$

The explicit expressions of the terms in Eq. (22) are given in the Appendix. After integration of Eq. (23), the matrix \mathbf{K}_M can be expressed as follows

$$\mathbf{K}_M = \mathbf{K}_M^a + \mathbf{K}_M^c + \mathbf{K}_M^b + \mathbf{K}_M^s \quad (24)$$

where \mathbf{K}_M^a is the axial stiffness matrix, \mathbf{K}_M^c the coupling stiffness matrix arising for the FGM material, \mathbf{K}_M^b the bending stiffness matrix, and \mathbf{K}_M^s the shearing stiffness matrix, of which the explicit expressions are given in the Appendix. The geometric stiffness matrix \mathbf{K}_G , the matrix

\mathbf{B}_m and the internal nodal force vector \mathbf{p} remains the same as those given by Felippa (2017), which are reproduced in the Appendix.

3. Numerical results

In the numerical study, geometrically non-linear deflections, namely, large deflections of the simple supported FGM beam are calculated and presented for different power-law exponents, porosity coefficients under a transversal point load (F) at the midpoint of the beam (Fig. 1). Also, geometrically linear and nonlinear results are presented and discussed for porosity effects. Using the conventional assembly procedure for the finite elements, the tangent stiffness matrix and the residual vector are obtained from the element stiffness matrices and residual vectors in the total Lagrangian sense. After that, the solution process outlined in the preceding section is used to obtain the solution for the problem of concern.

The FGM porous beam considered in numerical examples is made of metal material; Aluminum (Al; $E = 70$ GPa, $\nu = 0.3$) and ceramic material : Alumina (Al_2O_3 ; $E = 380$ GPa, $\nu = 0.3$). The bottom surface of the FGM beam is metal rich, whereas the top surface of the FGM beam is ceramic rich. When $k=0$ and $k=\infty$, the material of the beam gets homogeneous Alumina and homogeneous Aluminum, respectively, according to Eqs. (2) and (3). The dimensions of the beam are considered as follows: $b = 0.3$ m, $h = 0.3$ m, $L = 4$ m.

In order to obtain the optimum number of the finite element for the numerical calculations, the convergence study is performed in Fig. 5. In Fig. 5, nonlinear maximum vertical displacements (at the midpoint of the beam) of the FGM porous beam are calculated for different numbers of finite elements for the point load $F=200000$ kN, the power-law exponent $k=3$, the porosity parameter $a=0.2$ for uneven porosity model.

It is seen from Fig. 5 that the nonlinear maximum displacements converge perfectly after the finite element $n=60$. In order to obtain sensitive results, the number of finite elements is taken as 100 in the numerical calculations.

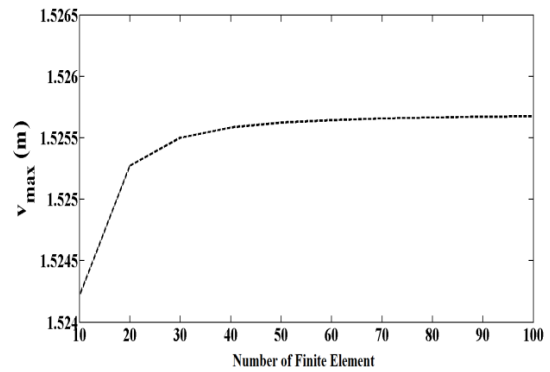


Fig. 5 Convergence study for nonlinear vertical displacements at the midpoint of the beam

Table 1 The effects of porosity and material graduation on the maximum vertical deflections of FGM porous beam in the linear and nonlinear analysis (meter).

Porosity Model	a	$k=0$		$k=0.5$		$k=1$		$k=8$	
		Linear	Nonlinear	Linear	Nonlinear	Linear	Nonlinear	Linear	Nonlinear
even porosity	0	0.5289	0.4960	0.8140	0.7176	1.0582	0.8753	1.7112	1.1675
	0.1	0.5622	0.5233	0.9022	0.7767	1.2292	0.9678	2.2561	1.3276
	0.2	0.5999	0.5534	1.0133	0.8456	1.4768	1.0811	3.5731	1.5521
uneven porosity	0	0.5289	0.4960	0.8140	0.7176	1.0582	0.8753	1.7112	1.1675
	0.1	0.5370	0.5027	0.8359	0.7329	1.1020	0.9007	1.8418	1.2137
	0.2	0.5453	0.5096	0.8594	0.7490	1.1509	0.9282	2.0082	1.2676

In Table 1, the maximum vertical deflections of the FGM porous beam are presented for different values of the porosity parameter (a), the power-law exponent (k) for different porosity models in both linear and nonlinear analysis for the point load $F=100000$ kN.

As can be seen from Table 1, the deflections of the beam increase with increase in the power-law exponents in both linear and nonlinear deflections. With increase in the k , the beam gets to full Aluminum. The Young modulus of the Aluminum is smaller than Alumina's. This is as expected, due to the fact that an increase in the k can increase the elasticity modulus and bending rigidity of the beam decrease according to Eqs. (2) and (3). As a result, the strength of the material increases. In addition, it is seen from Table 1 that increasing porosity parameter (a), yields increasing the deflections of the FGM beams, as expected. This is because, with increase in the porosity parameter, the intermolecular distances of the material increase and intermolecular forces decrease. As a result, the strength of the material decreases. Another result of Table 1 that the results of the even porosity model are bigger than uneven model's. It is mentioned before that, the rigidity of the beam in even porosity model is lower than the rigidity of the beam in uneven porosity model. So, the deflections in even porosity model are bigger than uneven model's.

In order to investigate the effect of porosity parameter (a) and porosity models on the geometrically linear and nonlinear responses of the FGM porous beam, the maximum transverse displacements obtained versus load rising (F) in Fig. 6 for the power-law exponent $k=3$.

As seen from Fig. 6, the displacements of the even porosity model are bigger than the displacements of uneven porosity model because the rigidity of the beam in even porosity model is lower than the rigidity of the beam in uneven porosity model. In Fig. 6(a), the results of the two models coincide with each other in case of $a=0$ because the porosity effect is not considered. Increase in porosity parameter a , the displacements increase considerably. Another result of Fig. 6 that the increase in load causes increase in difference between the displacement values of the linear and the nonlinear solutions. Increase in load is more effective in the vertical displacements and rotations of the linear solution. Also, the difference between FGM beam in the linear case is bigger than in the nonlinear's. This situation may be explained as follows: In the linear case, arm of the external forces or arm of the external resultant force do not change with the magnitude of the external

forces, and therefore the displacements depend on the external forces linearly. However, in the case of nonlinear analysis, the arm of the external forces change with the magnitude of the external force and, as the magnitude of the force increases the arm of these external forces decrease. However, as the forces increase the configuration of the FGM beam become close to vertical direction and therefore increase in the load does not cause a significant increase in displacements after certain load level in which the configuration of the beam is close to the vertical direction.

Fig. 7 displays the relationship between of porosity parameter a and the material distribution parameter k in the linear and nonlinear solution for two porosity models for the value of load $F=200000$ kN.

It is seen from Fig. 7 that increase in the k causes increase in the displacements. It is mentioned before that, with increase in the k , rigidity of the beam decrease according to Eqs. (2) and (3). Also, as seen from Fig. 7, the difference between the even and uneven porosity models increases with increase in k parameter. The difference of two models is quite large in the linear analysis. However, there is almost no difference in nonlinear analysis for two porosity models. It shows that the difference of the two models can be neglect in the nonlinear analysis. In the linear analysis, this difference is large to be. Another result of the Fig. 7 that the material distribution is very effective in the porosity effect. It can be concluded from here: with the suitable choice of parameter, the negative effects of the porosity can be reduced. It is observed from results that the material distribution plays an important role on the mechanical behaviour of the porous FGM beam.

Fig. 8 shows that the relationship between of porosity parameter a and the maximum displacements of the FGM porous beam in the geometrically linear and nonlinear analysis for $k=2$ and $F=200000$ kN. In Fig. 8, the porosity parameter k - maximum vertical displacements curves plotted for two porosity models.

It is seen from Fig. 8 that increase in the porosity parameter a , the difference between the even and uneven porosity models increases considerably. The difference between the even and uneven porosity models in the linear results is very large in comparison with the nonlinear results. The results of the linear analysis are bigger than the nonlinear's for all value of porosity parameters. Also, as seen from Fig. 8, the even porosity model is very sensitive in the linear analysis large in comparison with the nonlinear analysis and the results of the uneven model.

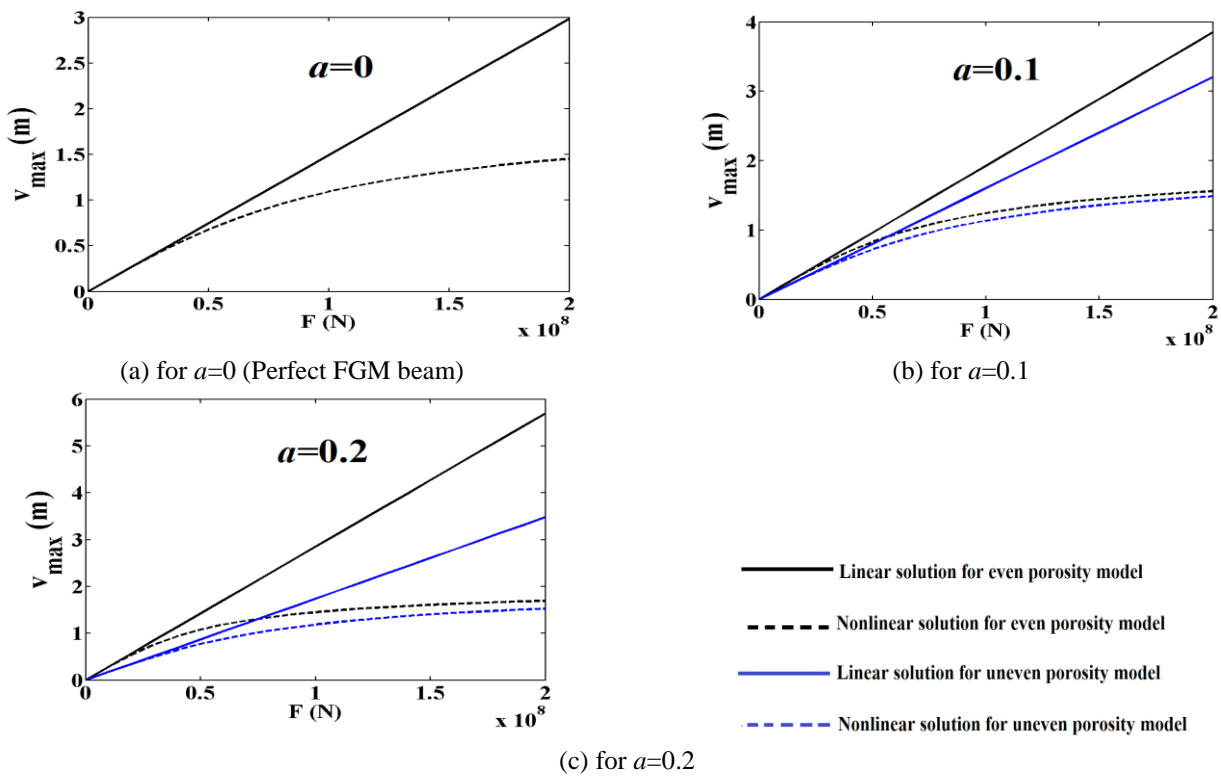


Fig. 6 Load-maximum vertical displacements curves for different the porosity parameter on the geometrically linear and nonlinear

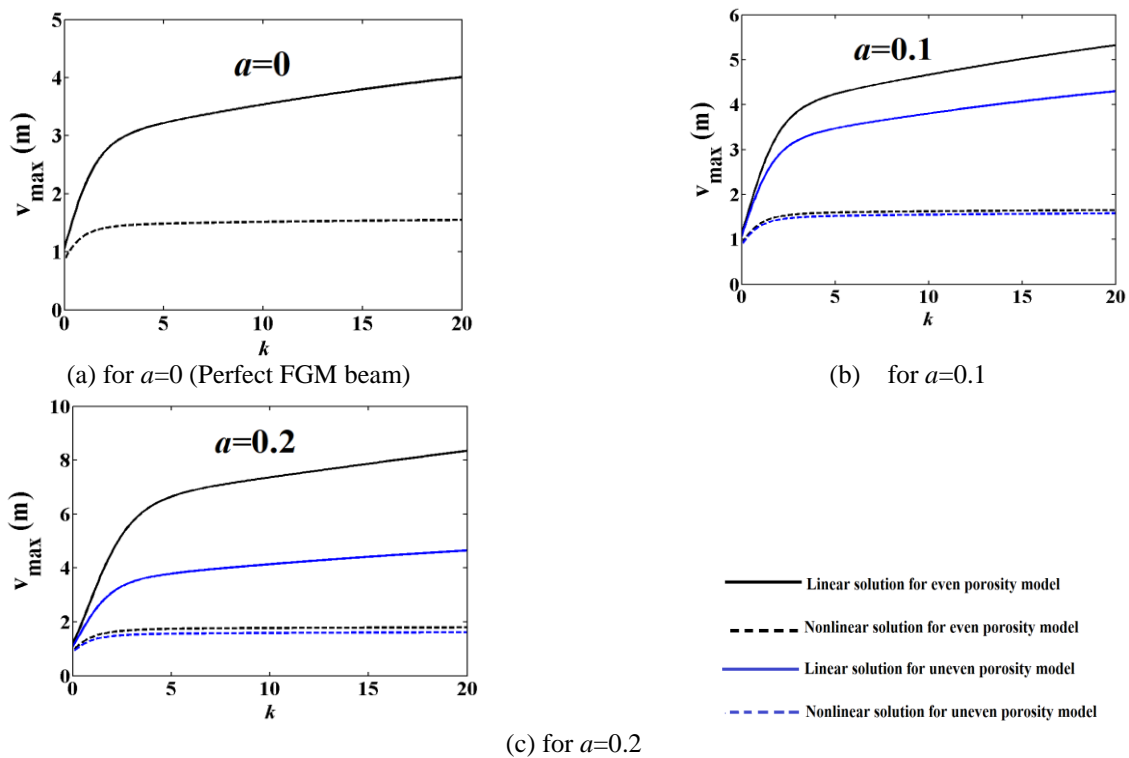


Fig. 7 The relationship between of porosity parameter a and the material distribution parameter k in the geometrically linear and nonlinear displacements of the FGM porous beam

However, uneven model display same characteristic feature in both linear and nonlinear solution. It shows that even and uneven models display different behavior in linear and nonlinear analysis.

Figs. 9 and 10 show that effect of material distribution parameter k on the deflected shape of the FGM porous beam for even and uneven porosity models, respectively for $a=0.2$ and $F=200000$ kN.

It is seen from Figs. 9 and 10 that different material distributions are very effective of the deflection of the beam. Increase in the k , the deflections of the FGM beam increase considerably. Also, the difference between the linear shape and the nonlinear shapes are displayed in Figs. 9 and 10. In the even porosity model, the beam more deflects in comparison with the uneven porosity model. In the nonlinear solution, the horizontal displacements of the FGM beam are high values because of geometrically nonlinear effect. However, the horizontal displacements are very small in the linear solution because the kinematic relations are based on initial position, so the displacements increase linearly.

Fig. 11 displays that effect of porosity parameter a on the deflected shape of the FGM porous beam for even and uneven porosity models in the linear and nonlinear case for $k=0.2$ and $F=200000$ kN.

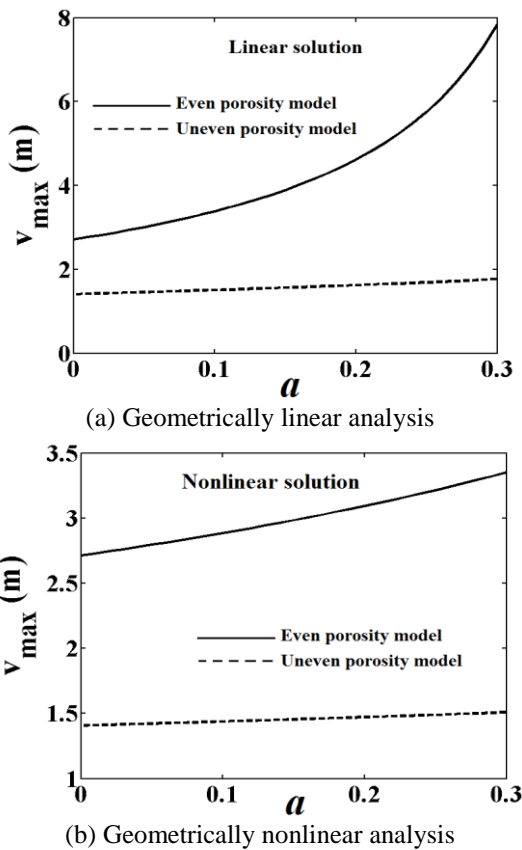


Fig. 8 The effect of porosity parameter (a) and porosity models on the geometrically linear and nonlinear displacements of the FGM porous beam

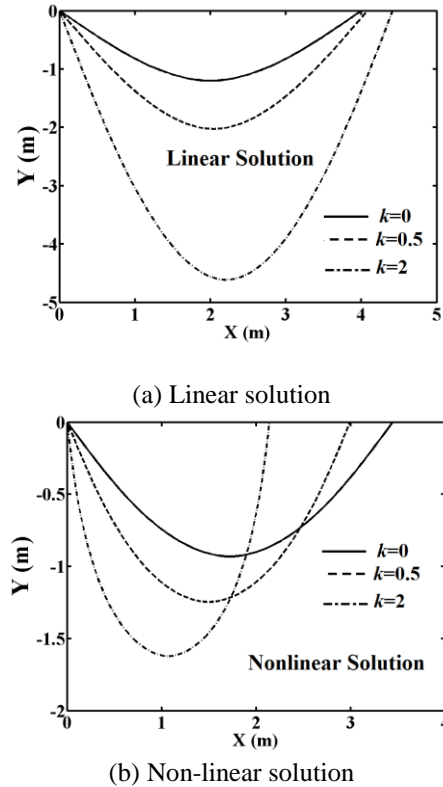


Fig. 9 The effect of material distribution parameter k on the deflected shape of the FGM porous beam for even porosity model

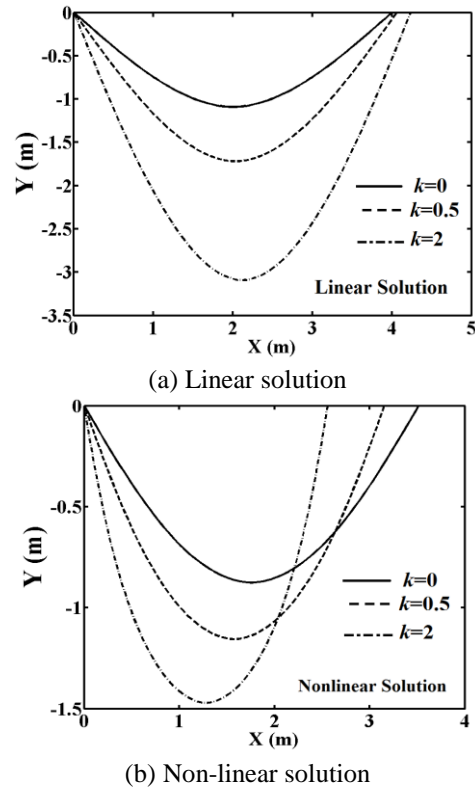


Fig. 10 The effect of material distribution parameter k on the deflected shape of the FGM porous beam for uneven porosity model

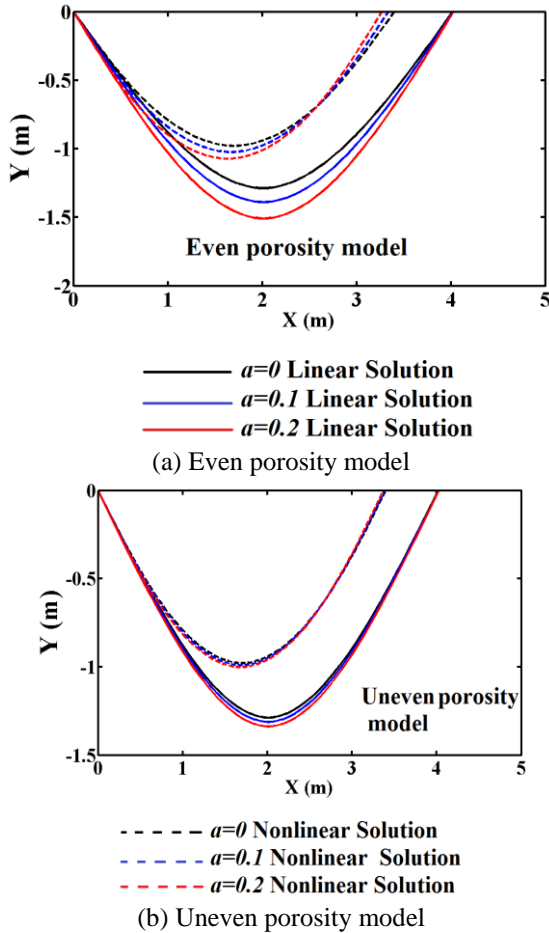


Fig. 11 The effect of porosity parameter a on the deflected shape of the FGM porous beam for linear and Non-linear case

As seen from Fig. 11, the differences of porosity parameters in the even porosity model are bigger than the uneven model's. Comparably, the differences of porosity parameters in the linear analysis are bigger than the nonlinear solution. It shows that porosity parameter play important role in the mechanical behavior of FGM beams.

4. Conclusions

Geometrically linear and nonlinear static responses of a FGM Timoshenko beam are investigated with porosity effect by using Total Lagrangian finite element method by taking into account full geometric nonlinearity. The effects of material distribution and porosity parameters on the deflections of the FGM porous beam are studied and discussed in both linear and nonlinear cases. The considered non-linear problem is solved by using incremental displacement-based finite element method in conjunction with Newton-Raphson iteration method. Convergence study was performed. The shortcomings of this study, the material nonlinearity and elasto-plastic behavior are not considered. It would be interesting to demonstrate the ability of the procedure through a wider campaign of investigations

concerning elasto-plastic or material nonlinear analysis of FGM porous beams with geometrically nonlinearity. From these results presented and discussed, the main conclusions are as follows:

- With increase in the power-law exponents leads to a rise on the deflections of the FGM beam in both linear and nonlinear deflections.
- With increase in porosity parameter, the deflections of the FGM beams increase considerably in both even and uneven porosity models.
- It is found that the deflections of the FGM beam by the even porosity are always larger than those by the uneven porosity models.
- With decrease in the power-law exponent, the difference between even and uneven porosity models decrease considerably.
- The porosity is very effective for the mechanical behavior of FGM porous beams.
- With the suitable choice of parameter, the negative effects of the porosity can be reduced.
- The porosity effect in the linear analysis is more sensitive than nonlinear analysis's. The difference between even porosity model and uneven porosity model can be neglect in the nonlinear analysis. In the linear analysis, this difference can not be neglected.
- The material distribution have a very important role on the mechanical behaviour of the FGM porous beam.

It is believed that the tabulated results will be a reference with which other researchers can compare their results.

References

- Agarwal, S., Chakraborty, A. and Gopalakrishnan, S. (2006), "Large deformation analysis for anisotropic and inhomogeneous beams using exact linear static solutions", *Compos. Struct.*, **72**(1), 91-104.
- Akbarzadeh Khorshidi, M., Shariati, M. and Emam, S.A. (2016), "Postbuckling of functionally graded nanobeams based on modified couple stress theory under general beam theory", *Int. J. Mech. Sci.*, **110**(1), 160-169.
- Akbaş, Ş.D. and Kocatürk, T. (2012), "Post-buckling analysis of Timoshenko beams with temperature-dependent physical properties under uniform thermal loading", *Struct. Eng. Mech.*, **44**(1), 109-125.
- Akbaş, Ş.D. and Kocatürk, T. (2013), "Post-buckling analysis of functionally graded three-dimensional beams under the influence of temperature", *J. Therm. Stresses*, **36**(12), 1235-1254.
- Akbaş, Ş.D. (2013a), "Geometrically nonlinear static analysis of edge cracked Timoshenko beams composed of functionally graded material", *Math. Probl. Eng.*, **2013**, 14.
- Akbaş, Ş.D. (2013b), "Free vibration characteristics of edge cracked functionally graded beams by using finite element method", *Int. J. Eng. Trends Technol.*, **4**(10), 4590-4597.
- Akbaş, Ş.D. (2014a), "Large post-buckling behavior of Timoshenko beams under axial compression loads", *Struct. Eng. Mech.*, **51**(6), 955-971.
- Akbaş, Ş.D. (2014b), "Free vibration of axially functionally graded beams in thermal environment", *Int. J. Eng. Appl. Sci.*, **6**(3), 37-51.
- Akbaş, Ş.D. (2015a), "On post-buckling behavior of edge cracked

- functionally graded beams under axial loads”, *Int. J. Struct. Stab. Dynam.*, **15**(4), 1450065.
- Akbaş, Ş.D. (2015b), “Post-buckling analysis of axially functionally graded three dimensional beams”, *Int. J. Appl. Mech.*, **7**(3), 1550047.
- Akbaş, Ş.D. (2015a), “Free vibration and bending of functionally graded beams resting on elastic foundation”, *Res. Eng. Struct. Mater.*, **1**(1).
- Akbaş, Ş.D. (2015b), “Large deflection analysis of edge cracked simple supported beams”, *Struct. Eng. Mech.*, **54**(3), 433-451.
- Akbaş, Ş.D. (2015c), “Wave propagation of a functionally graded beam in thermal environments”, *Steel Compos. Struct.*, **19**(6), 1421-1447.
- Akbaş, Ş.D. (2015d), “Free vibration and bending of functionally graded beams resting on elastic foundation”, *Res. Eng. Struct. Mater.*, **1**(1).
- Akbaş, Ş.D. (2017a), “Free vibration of edge cracked functionally graded microscale beams based on the modified couple stress theory”, *Int. J. Struct. Stab. Dynam.*, **17**(3), 1750033.
- Akbaş, Ş.D. (2017b), “Forced vibration analysis of functionally graded nanobeams”, *Int. J. Appl. Mech.*, **9**(7), 1750100.
- Akbaş, Ş.D. (2017c), “Post-buckling responses of functionally graded beams with porosities”, *Steel Compos. Struct.*, **24**(5), 579-589.
- Akbaş, Ş.D. (2017d), “Vibration and static analysis of functionally graded porous plates”, *J. Appl. Comput. Mech.*, **3**(3), 199-207.
- Akbaş, Ş.D. (2017e), “Nonlinear static analysis of functionally graded porous beams under thermal effect”, *Coupled Syst. Mech.*, **6**(4), 399-415.
- Akbaş, Ş.D. (2017f), “Stability of a non-homogenous porous plate by using generalized differential quadrature method”, *Int. J. Eng. Appl. Sci.*, **9**(2), 147-155.
- Akbaş, Ş.D. (2017g), “Thermal effects on the vibration of functionally graded deep beams with porosity”, *Int. J. Appl. Mech.*, **9**(5), 1750076.
- Akbaş, Ş.D. (2018a), “Forced vibration analysis of functionally graded porous deep beams”, *Compos. Struct.*, **186**, 293-302.
- Akbaş, Ş.D. (2018b), “Geometrically nonlinear analysis of a laminated composite beam”, *Struct. Eng. Mech.*, **66**(1), 27-36.
- Akbaş, Ş.D. (2018c), “Post-buckling responses of a laminated composite beam”, *Steel Compos. Struct.*, **26**(6), 733-743.
- Al Jahwari, F. and Naguib, H.E. (2016), “Analysis and homogenization of functionally graded viscoelastic porous structures with a higher order plate theory and statistical based model of cellular distribution”, *Appl. Math. Model.*, **40**(3), 2190-2205.
- Almeida, C.A., Albino, J.C.R., Menezes, I.F.M. and Paulino, G.H. (2011), “Geometric nonlinear analyses of functionally graded beams using a tailored Lagrangian formulation”, *Mech. Res. Commun.*, **38**(8), 553-559.
- Amara, K., Bouazza, M. and Fouad, B. (2016), “Postbuckling analysis of functionally graded beams using nonlinear model”, *Periodica Polytechnica. Eng., Mech. Eng.*, **60**(2), 121-128.
- Anand Rao, K.S., Gupta, R.K., Ramchandran, P. and Rao, V. (2010), “Thermal post-buckling analysis of uniform slender functionally graded material beams”, *Struct. Eng. Mech.*, **36**(5), 545-560.
- Atmane, H.A., Tounsi, A., Bernard, F. and Mahmoud, S.R. (2015a), “A computational shear displacement model for vibrational analysis of functionally graded beams with porosities”, *Steel Compos. Struct.*, **19**(2), 369-384.
- Atmane, H.A., Tounsi, A. and Bernard, F. (2015b), “Effect of thickness stretching and porosity on mechanical response of a functionally graded beams resting on elastic foundations”, *Int. J. Mech. Mater. Des.*, **13**(1), 71-84.
- Babilio, E. (2014), “Dynamics of functionally graded beams on viscoelastic foundation”, *Int. J. Struct. Stab. Dynam.*, **14**(8), 1440014, Doi: 10.1142/S0219455414400148.
- Bellifa, H., Benrahou, K.H., Hadji, L., Houari, M.S.A. and Tounsi, A. (2016), “Bending and free vibration analysis of functionally graded plates using a simple shear deformation theory and the concept the neutral surface position”, *J. Braz. Soc. Mech. Sci. Eng.*, **38**, 265-275.
- Benferhat, R., Daouadji, T.H., Mansour, M.S. and Hadji, L. (2016a), “Effect of porosity on the bending and free vibration response of functionally graded plates resting on Winkler-Pasternak foundations”, *Earthq. Struct.*, **10**(6), 1429-1449.
- Benferhat, R., Hassaine, D., Hadji, L. and Said, M. (2016b), “Static analysis of the FGM plate with porosities”, *Steel Compos. Struct.*, **21**(1), 123-136.
- Ebrahimi, F., Salari, E. and Hosseini, S.A.H. (2015), “Thermomechanical vibration behavior of FG nanobeams subjected to linear and non-linear temperature distributions”, *J. Therm. Stresses*, **38**(12), 1360-1386.
- Ebrahimi, F. and Salari, E. (2015a), “Effect of various thermal loadings on buckling and vibrational characteristics of nonlocal temperature-dependent FG nanobeams”, *Mech. Adv. Mater. Struct.*, 1-58.
- Ebrahimi, F. and Salari, E. (2015b), “Size-dependent thermo-electrical buckling analysis of functionally graded piezoelectric nanobeams”, *Smart Mater. Struct.*, **24**(12), 125007.
- Ebrahimi, F. and Salari, E. (2015), “A semi-analytical method for vibrational and buckling analysis of functionally graded nanobeams considering the physical neutral axis position”, *CMES Comput Model Eng Sci*, **105**(2), 151-181
- Ebrahimi, F. and Jafari, A. (2016a), “A higher-order thermomechanical vibration analysis of temperature-dependent FGM beams with porosities”, *J. Eng.*, **2016**, 20.
- Ebrahimi, F. and Jafari, A. (2016b), “Thermo-mechanical vibration analysis of temperature-dependent porous FG beams based on Timoshenko beam theory”, *Struct. Eng. Mech.*, **59**(2), 343-371.
- Ebrahimi, F., Ghasemi, F. and Salari, E. (2016), “Investigating thermal effects on vibration behavior of temperature-dependent compositionally graded Euler beams with porosities”, *Meccanica*, **51**(1), 223-249.
- Ebrahimi, F. and Habibi, S. (2016), “Deflection and vibration analysis of higher-order shear deformable compositionally graded porous plate”, *Steel Compos. Struct.*, **20**(1), 205-225.
- Ebrahimi, F. and Farzmandnia, N. (2016), “Thermo-mechanical vibration analysis of sandwich beams with functionally graded carbon nanotube-reinforced composite face sheets based on a higher-order shear deformation beam theory”, *Mech. Adv. Mater. Struct.*, 1-37
- Ebrahimi, F. and Barati, M.R. (2016a), “Dynamic modeling of a thermo-piezo-electrically actuated nanosize beam subjected to a magnetic field”, *Appl. Phys. A*, **122**(4), 1-18.
- Ebrahimi, F. and Barati, M.R. (2016b), “Vibration analysis of smart piezoelectrically actuated nanobeams subjected to magneto-electrical field in thermal environment”, *J. Vib. Control*, 1077546316646239.
- Ebrahimi, F. and Barati, M.R. (2016c), “Small scale effects on hygro-thermo-mechanical vibration of temperature dependent nonhomogeneous nanoscale beams”, *Mech. Adv. Mater. Struct.*, **24**(11), 924-936.
- Ebrahimi, F. and Hosseini, S.H.S. (2016), “Thermal effects on nonlinear vibration behavior of viscoelastic nanosize plates”, *J. Therm. Stresses*, **39**(5), 606-625.
- Elmaguiri, M., Haterbouch, M., Bouayad, A. and Oussouaddi, O. (2015), “Geometrically nonlinear free vibration of functionally graded beams”, *J. Mater. Environ. Sci.*, **6**(12), 3620-3633.
- Fallah, A. and Aghdam, M.M. (2011), “Nonlinear free vibration and post-buckling analysis of functionally graded beams on nonlinear elastic foundation”, *Eur. J. Mech.-A/Solids*, **30**(4), 571-583.

- Felippa, C.A. (2017), "Notes on nonlinear finite element methods", url: <http://www.colorado.edu/engineering/cas/courses.d/NFEM.d/NFEM.Ch11.d/NFEM.Ch11.pdf>.
- Galeban, M.R., Mojahedin, A., Taghavi, Y. and Jabbari, M. (2016), "Free vibration of functionally graded thin beams made of saturated porous materials", *Steel Compos. Struct.*, **21**(5), 999-1016.
- Hadji, L. and Bedia, E.A.A. (2015), "Influence of the porosities on the free vibration of FGM beams", *Wind Struct.*, **21**(3) 273-287.
- Hadji, L., Daouadji, T.H. and Bedia, E.A. (2015), "A refined exponential shear deformation theory for free vibration of FGM beam with porosities", *Geomech. Eng.*, **9**(3), 361-372.
- Hadji, L., Khelifa, Z. and Adda Bedia, E.A. (2016), "A new higher order shear deformation model for functionally graded beams", *KSCE J. Civil Eng.*, **20**(5), 1835-1841.
- Hadji, L. (2017), "Analysis of functionally graded plates using a sinusoidal shear deformation theory", *Smart Struct. Syst.*, **19**(4), 441-448.
- Hadji, L., Zouatnia, N. and Kassoul, A. (2017), "Wave propagation in functionally graded beams using various higher-order shear deformation beams theories", *Struct. Eng. Mech.*, **62**(2), 143-149.
- Hosseini, M. and Fazelzadeh, S.A. (2011), "Thermomechanical stability analysis of functionally graded thin-walled cantilever pipe with flowing fluid subjected to axial load", *Int. J. Struct. Stab. Dynam.*, **11**(3), 513-534.
- Hui-Shen, S. and Wang, Z.X. (2014), "Nonlinear analysis of shear deformable FGM beams resting on elastic foundations in thermal environments", *Int. J. Mech. Sci.*, **81**, 195-206.
- Jahwari, F. and Naguib, H.E. (2016), "Analysis and homogenization of functionally graded viscoelastic porous structures with a higher order plate theory and statistical based model of cellular distribution", *Appl. Math. Model.*, **40**(3), 2190-2205.
- Kolakowski, Z. and Teter, A. (2015), "Static interactive buckling of functionally graded columns with closed cross-sections subjected to axial compression", *Compos. Struct.*, **123**(1), 257-262.
- Kang, Y.A. and Li, X.F. (2009), "Bending of functionally graded cantilever beam with power-law non-linearity subjected to an end force", *Int. J. Nonlinear Mech.*, **44**(6), 696-703.
- Kang, Y.A. and Li, X.F. (2010), "Large deflections of a non-linear cantilever functionally graded beam", *J. Reinf. Plast. Comp.*, **29**(12), 1761-1774.
- Ke, L.L., Yang, J. and Kitipornchai, S. (2009), "Postbuckling analysis of edge cracked functionally graded Timoshenko beams under end shortening", *Compos. Struct.*, **90**(2), 152-160.
- Kocatürk, T. and Akbaş, Ş.D. (2010), "Geometrically non-linear static analysis of a simply supported beam made of hyperelastic material", *Struct. Eng. Mech.*, **35**(6), 677-697.
- Kocatürk, T. and Akbaş, Ş.D. (2011), "Post-buckling analysis of Timoshenko beams with various boundary conditions under non-uniform thermal loading", *Struct. Eng. Mech.*, **40**(3), 347-371.
- Kocatürk, T., Şimşek, M. and Akbaş, Ş.D. (2011), "Large displacement static analysis of a cantilever Timoshenko beam composed of functionally graded material", *Sci. Eng. Compos. Mater.*, **18**, 21-34.
- Kocatürk, T. and Akbaş, Ş.D. (2012), "Post-buckling analysis of Timoshenko beams made of functionally graded material under thermal loading", *Struct. Eng. Mech.*, **41**(6), 775-789.
- Kocatürk, T. and Akbaş, Ş.D. (2013), "Thermal post-buckling analysis of functionally graded beams with temperature-dependent physical properties", *Steel Compos. Struct.*, **15**(5), 481-505.
- Li, S.R., Zhang, J.H. and Zhao, Y.G. (2006), "Thermal post-buckling of functionally graded material Timoshenko beams", *Appl. Math. Mech. (English Edition)*, **26**(6), 803-810.
- Li, Q. and Li, S. (2011), "Post-buckling configuration of a functionally graded material column under distributed load", *Fuhe Cailiao Xuebao (Acta Materiae Compositae Sinica)*, **28**(3), 192-196.
- Li, L.Q. and Shao, Q.H. (2014), "Non-linear analysis of a FGM cantilever beam supported on a winkler elastic foundation", *Appl. Mech. Mater.*, **602**, 131-134.
- Mechab, I., Mechab, B., Benaïssa, S., Serier, B. and Bouiadjra, B.B. (2016a), "Free vibration analysis of FGM nanoplate with porosities resting on Winkler Pasternak elastic foundations based on two-variable refined plate theories", *J. Braz. Soc. Mech. Sci. Eng.*, **38**, 2193-2211.
- Mechab, B., Mechab, I., Benaïssa, S., Ameri, M. and Serier, B. (2016b), "Probabilistic analysis of effect of the porosities in functionally graded material nanoplate resting on Winkler-Pasternak elastic foundations", *Appl. Math. Model.*, **40**(2), 738-749.
- Mohanty, S.C., Dash, R.R. and Rout, T. (2012), "Static and dynamic stability analysis of a functionally graded Timoshenko beam", *Int. J. Struct. Stab. Dynam.*, **12**(4) Article ID 1250025, 33 pages.
- Mouaici, F., Benyoucef, S., Atmane, H.A. and Tounsi, A. (2016), "Effect of porosity on vibrational characteristics of non-homogeneous plates using hyperbolic shear deformation theory", *Wind Struct.*, **22**(4), 429-454.
- Nguyen, D.K., Gan, B.S. and Trinh, T.H. (2014), "Geometrically nonlinear analysis of planar beam and frame structures made of functionally graded material", *Struct. Eng. Mech.*, **49**(6) 727-743.
- Rastgo, A., Shafie, H. and Allahverdizadeh, A. (2005), "Instability of curved beams made of functionally graded material under thermal loading", *Int. J. Mech. Mater. Des.*, **2**, 117-128.
- Song, X. and Li, S. (2008), "Nonlinear stability of fixed-fixed FGM arches subjected to mechanical and thermal loads", *Adv. Mater. Res.*, **33-37**, 699-706.
- Sun, Y., Li, S.R. and Batra, R.C. (2016), "Thermal buckling and post-buckling of FGM mTimoshenko beams on nonlinear elastic foundation", *J. Therm. Stresses*, **39**(1), 11-26.
- Şimşek, M. and Aydın, M. (2017), "Size-dependent forced vibration of an imperfect functionally graded (FG) microplate with porosities subjected to a moving load using the modified couple stress Theory", *Compos. Struct.*, **160**, 408-421.
- Trinh, T.H., Nguyen, D.K., Gan, B.S. and Alexandrov, S. (2016), "Post-buckling responses of elastoplastic FGM beams on nonlinear elastic foundation", *Struct. Eng. Mech.*, **58**(3), 515-532.
- Wattanasakulpong, N. and Ungbhakorn, V. (2014), "Linear and nonlinear vibration analysis of elastically restrained ends FGM beams with porosities", *Aerosp. Sci. Technol.*, **32**(1), 111-120.
- Yahia, S.A., Atmane, H.A., Houari, M.S.A. and Tounsi, A. (2015), "Wave propagation in functionally graded plates with porosities using various higher-order shear deformation plate theories", *Struct. Eng. Mech.*, **53**(6), 1143-1165.
- Yan, T., Yang, J. and Kitipornchai, S. (2012), "Nonlinear dynamic response of an edge-cracked functionally graded Timoshenko beam under parametric excitation", *Nonlinear Dynam.*, **67**(1), 527-540.
- Zhang, D.G. and Zhou, H.M. (2014), "Nonlinear bending and thermal post-buckling analysis of FGM beams resting on nonlinear elastic foundations", *CMES Comput. Model. Eng.*, **100**(3) 201-222.
- Zouatnia, N., Hadji, L. and Kassoul, A. (2017), "An analytical solution for bending and vibration responses of functionally graded beams with porosities", *Wind Struct.*, **25**(4), 329-342.

Appendix

In this Appendix, the entries of the following matrices are given: axial stiffness matrix \mathbf{K}_M^a , coupling stiffness matrix \mathbf{K}_M^c arising for the FGM, bending stiffness matrix \mathbf{K}_M^b , and shearing stiffness matrix \mathbf{K}_M^s Felippa (2017).

$$\mathbf{K}_M^a = \frac{A_{XX}}{L_0} \begin{bmatrix} c_m^2 & c_m s_m & -c_m \gamma_m L_0/2 & -c_m^2 & -c_m s_m & -c_m \gamma_m L_0/2 \\ c_m s_m & s_m^2 & -s_m \gamma_m L_0/2 & -c_m s_m & -s_m^2 & -s_m \gamma_m L_0/2 \\ -c_m \gamma_m L_0/2 & -s_m \gamma_m L_0/2 & \gamma_m^2 L_0^2/4 & c_m \gamma_m L_0/2 & -s_m \gamma_m L_0/2 & \gamma_m^2 L_0^2/4 \\ -c_m^2 & -c_m s_m & c_m \gamma_m L_0/2 & c_m^2 & c_m s_m & c_m \gamma_m L_0/2 \\ -c_m s_m & -s_m^2 & s_m \gamma_m L_0/2 & c_m s_m & s_m^2 & s_m \gamma_m L_0/2 \\ c_m \gamma_m L_0/2 & -s_m \gamma_m L_0/2 & \gamma_m^2 L_0^2/4 & c_m \gamma_m L_0/2 & s_m \gamma_m L_0/2 & \gamma_m^2 L_0^2/4 \end{bmatrix} \quad (A1)$$

$$\mathbf{K}_M^c = \frac{B_{XX}}{L_0} \begin{bmatrix} 0 & 0 & -c_m & 0 & 0 & c_m \\ 0 & 0 & -s_m & 0 & 0 & s_m \\ -c_m & -s_m & \gamma_m L_0 & c_m & s_m & 0 \\ 0 & 0 & c_m & 0 & 0 & -c_m \\ 0 & 0 & s_m & 0 & 0 & -s_m \\ c_m & s_m & 0 & -c_m & -s_m & -\gamma_m L_0 \end{bmatrix} \quad (A2)$$

$$\mathbf{K}_M^b = \frac{D_{XX}}{L_0} \begin{bmatrix} 0 & 0 & 0 & 0 & 0 & 0 \\ 0 & 0 & 0 & 0 & 0 & 0 \\ 0 & 0 & 1 & 0 & 0 & -1 \\ 0 & 0 & 0 & 0 & 0 & 0 \\ 0 & 0 & 0 & 0 & 0 & 0 \\ 0 & 0 & -1 & 0 & 0 & 1 \end{bmatrix} \quad (A3)$$

$$\mathbf{K}_M^s = \frac{A_{XZ}}{L_0} \begin{bmatrix} s_m^2 & -c_m s_m & \frac{-s_m \alpha_1 L_0}{2} & -s_m^2 & c_m s_m & \frac{-s_m \alpha_1 L_0}{2} \\ -c_m s_m & c_m^2 & \frac{c_m \alpha_1 L_0}{2} & c_m s_m & -c_m^2 & \frac{c_m \alpha_1 L_0}{2} \\ \frac{-s_m \alpha_1 L_0}{2} & \frac{c_m \alpha_1 L_0}{2} & \frac{\alpha_1^2 L_0^2}{4} & \frac{s_m \alpha_1 L_0}{2} & \frac{-c_m \alpha_1 L_0}{2} & \frac{\alpha_1^2 L_0^2}{4} \\ -s_m^2 & c_m s_m & \frac{s_m \alpha_1 L_0}{2} & s_m^2 & -c_m s_m & \frac{s_m \alpha_1 L_0}{2} \\ c_m s_m & -c_m^2 & \frac{-c_m \alpha_1 L_0}{2} & -c_m s_m & c_m^2 & \frac{-c_m \alpha_1 L_0}{2} \\ \frac{-s_m \alpha_1 L_0}{2} & \frac{c_m \alpha_1 L_0}{2} & \frac{\alpha_1^2 L_0^2}{4} & \frac{s_m \alpha_1 L_0}{2} & \frac{-c_m \alpha_1 L_0}{2} & \frac{\alpha_1^2 L_0^2}{4} \end{bmatrix} \quad (A4)$$

where m denotes the midpoint of the beam, $\xi=0$, and $\theta_m = (\theta_1 + \theta_2)/2$, $\omega_m = \theta_m + \varphi$, $c_m = \cos \omega_m$, $s_m = \sin \omega_m$,

$$e_m = \frac{L \cos(\theta_m - \psi)}{L_0} - 1, \quad \alpha_1 = 1 + e_m \quad \text{and} \quad \gamma_m = \frac{L \cos(\psi - \theta_m)}{L_0}$$

(See Fig. A1 for symbols). The initial axis of the beam considered is taken as horizontal, therefore $\varphi=0$. The matrix \mathbf{S} is defined as follows

$$\mathbf{S} = \begin{bmatrix} A_{XX} & 0 & -B_{XX} \\ 0 & A_{XZ} & 0 \\ -B_{XX} & 0 & D_{XX} \end{bmatrix} \quad (A5)$$

The matrix \mathbf{B}_m is given as follows

$$\mathbf{B}_m = \mathbf{B}_m|_{\xi=0} = \frac{1}{L_0} \begin{bmatrix} -c_m & -s_m & -\frac{1}{2} L_0 \gamma_m & c_m & s_m & -\frac{1}{2} L_0 \gamma_m \\ s_m & -c_m & \frac{1}{2} L_0 (1 + e_m) & s_m & -c_m & \frac{1}{2} L_0 (1 + e_m) \\ 0 & 0 & -1 & 0 & 0 & 1 \end{bmatrix} \quad (A6)$$

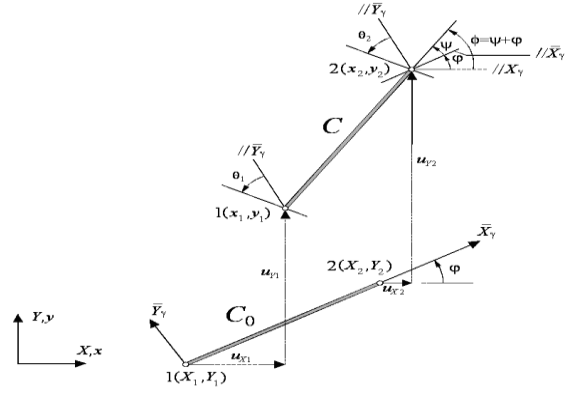


Fig. A1 Plane beam element with arbitrarily oriented reference configuration Felippa (2017)

The geometric stiffness matrix K_G is given as follows

$$\mathbf{K}_G = \frac{N_m}{2} \begin{bmatrix} 0 & 0 & s_m & 0 & 0 & s_m \\ 0 & 0 & -c_m & 0 & 0 & -c_m \\ s_m & -c_m & -\frac{1}{2} L_0 (1 + e_m) & -s_m & c_m & -\frac{1}{2} L_0 (1 + e_m) \\ 0 & 0 & -s_m & 0 & 0 & -s_m \\ 0 & 0 & c_m & 0 & 0 & c_m \\ s_m & -c_m & -\frac{1}{2} L_0 (1 + e_m) & -s_m & c_m & -\frac{1}{2} L_0 (1 + e_m) \end{bmatrix} \quad (A7)$$

$$+ \frac{V_m}{2} \begin{bmatrix} 0 & 0 & c_m & 0 & 0 & c_m \\ 0 & 0 & s_m & 0 & 0 & s_m \\ c_m & s_m & -\frac{1}{2} L_0 \gamma_m & -c_m & -s_m & -\frac{1}{2} L_0 \gamma_m \\ 0 & 0 & -c_m & 0 & 0 & -c_m \\ 0 & 0 & -s_m & 0 & 0 & -s_m \\ c_m & s_m & -\frac{1}{2} L_0 \gamma_m & -c_m & -s_m & -\frac{1}{2} L_0 \gamma_m \end{bmatrix}$$

in which N_m and V_m are the axial and shear forces evaluated at the midpoint. The internal nodal force vector is Felippa (2017)

$$\mathbf{p} = L_0 \mathbf{B}_m^T \mathbf{z} = \begin{bmatrix} -c_m & -s_m & -\frac{1}{2} L_0 \gamma_m & c_m & s_m & \frac{1}{2} L_0 \gamma_m \\ s_m & -c_m & -\frac{1}{2} L_0 (1 + e_m) & s_m & -c_m & -\frac{1}{2} L_0 (1 + e_m) \\ 0 & 0 & -1 & 0 & 0 & 1 \end{bmatrix}^T \begin{bmatrix} N \\ V \\ M \end{bmatrix} \quad (A8)$$

where $\mathbf{z}^T = [N \quad V \quad M]$. The external nodal force is

$$\mathbf{f} = b \int_h \int_{L_0} \begin{bmatrix} 1 - \xi_1 & 0 & 0 \\ 0 & 1 - \xi_1 & 0 \\ 0 & 0 & 1 - \xi_1 \\ 1 - \xi_2 & 0 & 0 \\ 0 & 1 - \xi_2 & 0 \\ 0 & 0 & 1 - \xi_2 \end{bmatrix} \begin{bmatrix} f_x \\ f_y \\ 0 \end{bmatrix} dXdY \quad (A9)$$

$$+ b \int_{L_0} \int_h \int_{L_0} \begin{bmatrix} 1 - \xi_1 & 0 & 0 \\ 0 & 1 - \xi_1 & 0 \\ 0 & 0 & 1 - \xi_1 \\ 1 - \xi_2 & 0 & 0 \\ 0 & 1 - \xi_2 & 0 \\ 0 & 0 & 1 - \xi_2 \end{bmatrix} \begin{bmatrix} t_x \\ t_y \\ m_z \end{bmatrix} dXdY$$

where f_x , f_y are the body forces, t_x , t_y , m_z are the surface loads in the X , Y directions and about the Z axis.